Adsorption (2008) 14: 181–188
DOI 10.1007/s10450-007-9075-8

Isomerization kinetics of small hydrocarbons in confinement

Erik E. Santiso · Marco Buongiorno Nardelli · Keith E. Gubbins

Received: 4 May 2007 / Revised: 10 August 2007 / Accepted: 22 October 2007 / Published online: 8 November 2007

Abstract Chemical reactions are often carried out in nanostructured materials, which can enhance reactions due to their large specific surface area, their interactions with the reacting mixture and confinement effects. In this work, we present a systematic study of the effect that the geometrical restrictions imposed by the pore walls can have on reactions that involve a three dimensional rearrangement of the atoms in a molecule. In particular, we consider the isomerization of three 4-membered hydrocarbons—n-butane, 1-butene and 1,3-butadiene confined in carbon nanopores of slit geometry. Our results illustrate the fact that, in the molecular sieving limit, the reaction rates change as the double exponential of the pore size (Santiso et al., in J. Chem. Phys., 2007a, submitted), and therefore the transition rates in nanopores can be many orders of magnitude different from the corresponding bulk values. These results can be used as a guideline for the molecular-level design of improved catalytic materials.

E.E. Santiso (✉) · K.E. Gubbins
Department of Chemical Engineering, North Carolina State University, Raleigh, NC 27695, USA
e-mail: eesantis@unity.ncsu.edu

M. Buongiorno Nardelli
Department of Physics, North Carolina State University, Raleigh, NC 2769, USA

M. Buongiorno Nardelli
CCS-CSM, Oak Ridge National Laboratory, Oak Ridge, TN 37831, USA

E.E. Santiso · M. Buongiorno Nardelli · K.E. Gubbins
Center for High-Performance Simulation (CHiPS), North Carolina State University, Raleigh, NC 27695, USA

Keywords Chemical reactions · Confinement · Carbon · Density functional theory · Variational transition state theory

Abbreviations

A	Frequency factor
A'	Scaled frequency factor, $A' \equiv A \exp(-\Delta E^{\ddagger}_{\infty}/k_B T)$
a.u.	Atomic unit (for length, 1 a.u. = 1 Bohr radius = 0.5291772108 Å)
E_{ov}	Energy due to the overlap of the electron clouds
k	Rate constant
k_{∞}	Rate constant for a reaction occurring in the bulk phase
k_B	Boltzmann's constant ($1.3806503 \times 10^{-23}$ J/K)
P	Overlap energy parameter
P'	Scaled overlap energy parameter, $P' \equiv P/k_B T$
r	Pore width
R^2	Pearson's correlation coefficient squared
T	Absolute temperature (K)
$\Delta E^{\ddagger}$	Activation energy barrier
$\Delta E^{\ddagger}_{\infty}$	Activation energy barrier for a reaction occurring in the bulk phase
ρ	Molecular size parameter

1 Introduction

Chemical reactions are often carried out in nano-structured materials, which can enhance reaction rates and equilibrium yields through many different effects. Some of these effects include an increase in the contact area between the catalyst and the reactive mixture, additional catalytic effects due to interactions with the support, selective adsorption of the reactants and/or products, and geometric constraints, among others. An understanding of the individual role of each one

of these effects could be used to systematically design improved catalytic materials that take advantage of all of them. Experimental measurements, however, often reflect an integration over many of these effects, which makes it challenging to interpret the results. The difficulties and costs associated with a purely experimental approach make this problem a good candidate for simulation studies.

Despite the multitude of particular effects that can influence chemical reactions in confinement, they are ultimately a consequence of one or more of three factors: (1) The effect of the shape of the confining material and/or the reduced dimensionality of the porous space, which we term the "shape-catalytic" effect; (2) Physical interactions with the confining material, e.g. electrostatic and dispersion interactions; and (3) Chemical interactions, i.e. interactions that involve electron rearrangement and/or the formation of chemical bonds with the confining material. The latter effect is the one most often studied, as it has the most patent influence on reaction rates. The other two effects, however, can have a significant impact on the rates and equilibrium yields of many chemical reactions, as discussed in several recent experimental (Byl et al. 2003; Kaneko et al. 1989; Imai et al. 1991) and theoretical (Lisal et al. 2006; Travis and Searles 2006; Halls and Schlegel 2002; Santiso et al. 2005a, 2005b, 2006, 2007a, 2007b; Turner and Gubbins 2003; Turner et al. 2001a, 2001b, 2002) studies.

Our recent work has been focused on understanding the relative impact of the different effects mentioned above on reactions happening within graphitic carbon pores and nanostructures (Santiso et al. 2005a, 2005b, 2006, 2007a, 2007b; Kostov et al. 2005). Our choice of carbon as the confining material is due to several reasons: (1) A detailed study of chemical reactions often requires the use of *ab initio* methods, since reactions involve changes in the electronic states of the atoms involved. Graphitic carbon is a relatively simple material to model, which allows us to explore different reactions and wider parameter spaces without a huge computational expense; (2) Graphitic carbon can be shaped into many different structures (Dresselhaus et al. 1995; Bandow et al. 2000; Berber et al. 2000; Bandosz et al. 2003), which makes it a good candidate for studies of the shape-catalytic effect; (3) The chemical reactivity of a carbon support can be modified by the inclusion of structural defects (Hashimoto et al. 2004; El-Barbary 2005; Kostov et al. 2005), the addition of functional groups and/or doping (Dresselhaus et al. 1995). This allows us to study the influence of different types of chemical interactions in a systematic way; and (4) Graphitic carbon has a large polarizability, which makes it suitable for the study of physical interactions and their effect on chemical reactions.

In a recent paper (Santiso et al. 2007a) we considered the effect of the shape and size of the confining material on the potential energy barriers of three 4-membered hydrocarbons: n-butane, 1-butene and 1,3-butadiene. We showed that confinement within pores of sub-nanometer size has a tremendous impact on the energy barriers for the isomerization reactions between the different stable molecular conformations of these hydrocarbons. We also considered the kinetics of the *anti-gauche* transition of n-butane using Transition State Theory (TST) (see, e.g. Simons 2003), and showed that, in the molecular sieving limit, the rate of this transition changes as the double exponential of the pore size—with the rate changing over tens of orders of magnitude within a range of pore sizes of a couple of Angstroms. If such an effect could be systematically exploited, it would be possible to design much improved catalytic materials by controlling the dimensions of the pores.

In this work we present a more detailed study of the isomerization kinetics of all three of the hydrocarbons mentioned above, and show that the double exponential effect indeed appears in all the cases. We also discuss the applicability of the double-exponential theory to general chemical reactions.

2 Methods

The torsional energy profiles of n-butane, 1-butene and 1,3-butadiene were obtained using plane-wave pseudopotential density functional theory (DFT) (Parr and Yang 1989; Santiso and Gubbins 2004), using the Becke-Lee-Yang-Parr (BLYP) exchange-correlation functional (Becke 1988; Lee et al. 1988) and ultrasoft pseudopotentials (Vanderbilt 1990). The calculations were carried out using the CPMD package (CPMD, Copyright IBM Corp 1990–2006, Copyright MPI für Festkörperforschung Stuttgart 1997–2001, http://www.cpmd.org).

The torsional profiles were obtained by performing a set of structural relaxations with the four carbon atoms constrained to different dihedral angles. Then we relaxed the stable states, and optimized the transition state structures using the partitioned rational function optimization (P-RFO) method (Banerjee et al. 1985; Billeter et al. 2003). For some of the smaller pore sizes, we performed additional constrained optimizations around the transition state region in order to obtain reliable estimates of the transition barrier. This was necessary because, in the smaller pores, the detailed structure of the carbon walls becomes important and there are many local minima and saddle points depending on the relative position of the molecule above the carbon lattice. The calculations were carried out for a free molecule (to represent a bulk ideal gas), and molecules confined within pores of decreasing physical pore widths down to 0.58 nm (our original calculations were done in atomic units, with pore sizes between 11 a.u. and 15 a.u. in steps of 1 a.u. Since the atomic unit is not in widespread use in the adsorption literature, we report the pore widths in nm throughout the paper).

The carbon walls were modeled as 32-atom graphene sheets with the atoms constrained to their equilibrium lattice positions, as found in a previous unit cell relaxation. We examined the effect of the unit cell size and the structural constraints on the torsional potentials, and found that the changes were negligible compared to the effect of confinement. We also considered the addition of an empirical van der Waals correction to account for dispersion forces, but did not find a significant effect—at the pore sizes considered, the steric (overlap) interaction is by far the dominant effect. More details on the energetics are given in our previous paper (Santiso et al. 2007a).

We also estimated the rate constant for the asymmetric isomerization of all three hydrocarbons using Variational Transition State Theory (VTST) (see, e.g. Simons 2003). For this we ran phonon calculations at all the different structures and calculated the molecular partition function of the free molecule (in the bulk calculations) or the confined molecule (in the pore calculations) at the given geometry using the ParFuMS code (Partition Functions of Molecules and Solids, E.E. Santiso, 2007, http://gubbins.ncsu.edu/users/erik/parfums/; Reed and Gubbins 1973; Gray and Gubbins 1984). For the 'activated' (i.e. nonequilibrium) conformations, we projected out the reactive mode as obtained from the equation defining the torsional constraint (Page and McIver 1988; González et al. 2004; Santiso and Gubbins, in preparation). The partition function was then used to obtain the free energy as a function of temperature at all conformations and pore widths in the ideal gas limit (in the bulk) or Henry's law limit (in the pores). We then splined the data at each temperature as a function of the torsion angle, located the maximum of the activation free energy barrier, and used it to calculate the VTST rate constant.

3 Results and discussion

The full details of the energy profiles of n-butane, 1-butene, and 1,3-butadiene have been given elsewhere (Santiso et al. 2007a, 2007b). Here we review only the results that are relevant to this work. Table 1 lists the stable conformers found in the bulk and within slit pores of widths ranging from 0.58 nm to 0.74 nm. The dihedral angle (in degrees) between the four carbon atoms in the molecule is given in Table 1 below its name. Figure 1 shows snapshots of the various molecular conformations to aid in visualization.

For n-butane, the global minimum both in the bulk and within the pores is an *anti* conformer, with the methyl end groups pointing away from each other at 180°. The geometry of the high-energy conformer, however, changes with decreasing pore width because the steric hindrance imposed by the pore walls favors the planar conformations. Thus, the *gauche* conformation at 65.0° is first changed to a more planar *gauche* conformation at 38.9° within the pore of width 0.74 nm, and below this pore width the *syn* conformer, at 0°, becomes stable.

For 1-butene, the global energy minimum in the bulk is a *skew* conformer, with a C-C-C-C dihedral angle of 121.2°. As is the case with the *gauche* conformer of n-butane, this non-planar conformation interacts strongly with the pore walls and the torsion angle within the pore drifts toward the planar *anti* conformation at 180° as pore size decreases. The high-energy conformer in the bulk, with a *syn* geometry (0°), actually becomes the energy minimum within the pores, as it has a lower steric hindrance between the methyl and methylene end groups than the distorted *skew* and *anti* conformers.

The trends seen in 1,3-butadiene are similar to the ones shown for n-butane: both in the bulk and within the pores

Table 1 Stable conformers of n-butane, 1-butene, and 1,3-butadiene in the bulk and within carbon slit pores. The C-C-C-C dihedral angle for each conformer is given in parenthesis below its name

Molecule →	n-Butane		1-Butene		1,3-Butadiene	
Pore width ↓	Global minimum	High-energy conformer	Global minimum	High-energy conformer	Global minimum	High-energy conformer
Bulk (∞)	*anti*	*gauche*	*skew*	*syn*	*s-trans*	*gauche*
	(180°)	(65.0°)	(121.2°)	(0°)	(180°)	(30.3°)
0.74 nm	*anti*	*gauche*	*syn*	*skew*	*s-trans*	*gauche*
	(180°)	(38.9°)	(0°)	(148.1°)	(180°)	(19.7°)
0.69 nm	*anti*	*syn*	*syn*	*skew*	*s-trans*	*s-cis*
	(180°)	(0°)	(0°)	(167.4°)	(180°)	(0°)
0.64 nm	*anti*	*syn*	*syn*	*anti*	*s-trans*	*s-cis*
	(180°)	(0°)	(0°)	(180°)	(180°)	(0°)
0.58 nm	*anti*	*syn*	*syn*	*anti*	*s-trans*	*s-cis*
	(180°)	(0°)	(0°)	(180°)	(180°)	(0°)

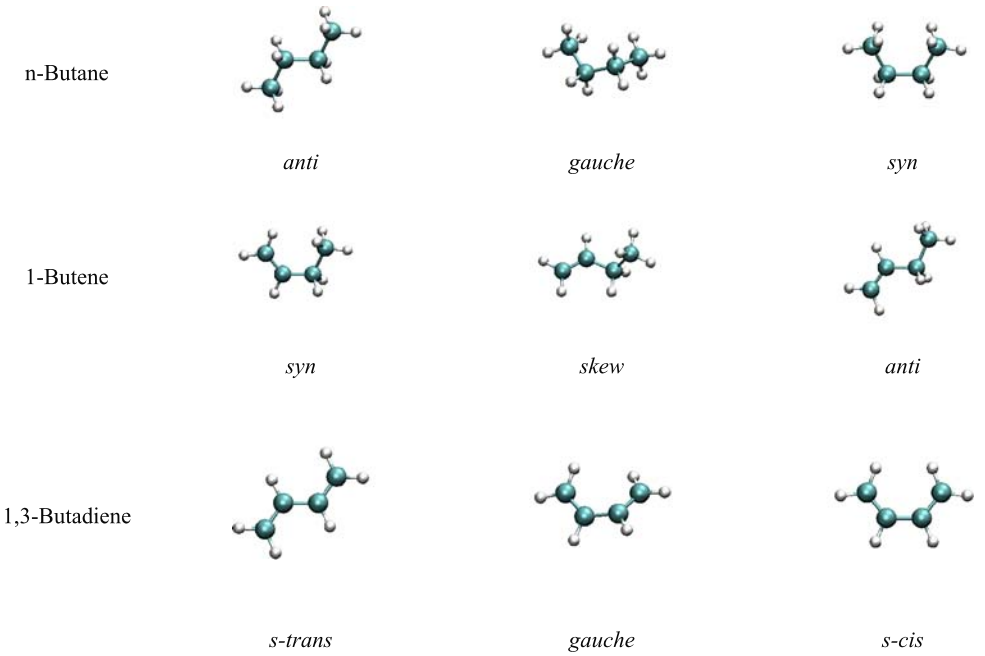

Fig. 1 Snapshots of the stable conformers of n-butane, 1-butene, and 1,3-butadiene as obtained from our DFT calculations. The non-planar conformations given correspond to the bulk molecules

the global energy minimum corresponds to an *s-trans* conformation, with both methylene groups pointing away from each other at 180°. A *gauche* conformer, with a C-C-C-C dihedral angle of 30.3°, is the stable conformer in the bulk. The lower torsion angle (as compared to n-butane) is due to the additional energy penalty of breaking the conjugated bond in 1,3-butadiene. As in the previous cases, the non-planar *gauche* conformation interacts more strongly with the pore walls: its torsion angle is first decreased to 19.7° in the 0.74 nm pore, and then the *s-cis* planar conformation, at 0°, becomes stable.

The reactions considered in this work are the asymmetric conformational transitions, i.e. the transitions between conformers of different geometries, as opposed to the automerization reactions between identical conformers (e.g. the *gauche* → *gauche* automerization in bulk n-butane passing through a *syn* transition state). The latter are more suited to direct molecular dynamics (MD) studies (Frenkel and Smit 2002; Travis and Searles 2006; Brown and Clarke 1990a, 1990b), as their energy barriers, especially within the pores, are low enough for reactive events to be seen in such simulations (The asymmetric transition rates in the bulk would be accessible to such an approach. Since the rate constants decrease dramatically in the pore sizes considered here we preferred, however, to be consistent and use Variational Transition State Theory also in the bulk. The error introduced by this is certainly negligible compared to the observed effect of confinement). In Table 2 we list the reactions that we studied, and give the corresponding activation energy barriers in the bulk and within the pores. We also show the C-C-C-C dihedral angle (in degrees) corresponding to the transition state structure in each case.

As shown in Table 2, the transition state for all the asymmetric transitions considered is non-planar, and thus its energy is greatly increased with decreasing pore size due to the steric hindrance imposed by the pore walls. This causes the activation energy barriers to increase rapidly with decreasing pore size, especially in the narrowest pores. As discussed below, this has a very large impact on the kinetics of these reactions.

Figure 2 shows three sets of Arrhenius plots for the rates of all the isomerization reactions listed in Table 2, as obtained from our VTST calculations. From these figures it is evident that confinement has a dramatic impact on the reaction rates—in all cases, the plots span more than 30 orders of magnitude. As an example, the characteristic time (inverse of the rate constant) for the asymmetric isomerization (*anti* → *gauche*/*anti* → *syn*) of n-butane at 300 K changes from 64 ps in the bulk to 0.9 million years within the 0.58 nm pore—a change of over 25 orders of magnitude. The dependence of the rate on pore width is also quite extreme at the smaller pore sizes—the characteristic time for the same reaction within the 0.74 nm pore at 300 K is 8 ns, so the rate changes by more than 23 orders of magnitude within a range of pore sizes of only 0.16 nm.

Similar results are obtained for 1-butene, although the more drastic changes happen at smaller pore sizes compared to n-butane, reflecting the fact that 1-butene is a smaller molecule. Nevertheless, the variation of the rate with pore size is still quite extreme—for example, the characteristic time for the asymmetric isomerization (*syn* → *skew*/*syn* → *anti*) changes from an estimated 2 ps in the bulk to 0.27 ns in the 0.74 nm-wide pore and to 430 years in the

Table 2 Asymmetric reactions considered in this work and their corresponding activation barriers ($\Delta E^{\ddagger}$) in the bulk and within carbon slit pores. The C-C-C-C dihedral at the transition state conformation is given in parenthesis below the reaction

Molecule →	n-Butane		1-Butene		1,3-Butadiene	
Pore width ↓	Reaction (TS angle)	$\Delta E^{\ddagger}$ (kcal/mol)	Reaction	$\Delta E^{\ddagger}$ (kcal/mol)	Reaction	$\Delta E^{\ddagger}$ (kcal/mol)
Bulk (∞)	*anti*→*gauche* (118.6°)	3.1	*syn*→*skew* (54.4°)	1.8	*s-trans*→*gauche* (99.5°)	7.5
0.74 nm	*anti*→*gauche* (116.4°)	8.5	*syn*→*skew* (81.8°)	5.2	*s-trans*→*gauche* (97.4°)	9.5
0.69 nm	*anti*→*syn* (116.6°)	14.6	*syn*→*skew* (85.3°)	10.0	*s-trans*→*s-cis* (97.5°)	13.1
0.64 nm	*anti*→*syn* (108.2°)	25.1	*syn*→*anti* (93.6°)	17.9	*s-trans*→*s-cis* (99.9°)	18.7
0.58 nm	*anti*→*syn* (118.8°)	38.5	*syn*→*anti* (102.5°)	30.5	*s-trans*→*s-cis* (102.0°)	29.5

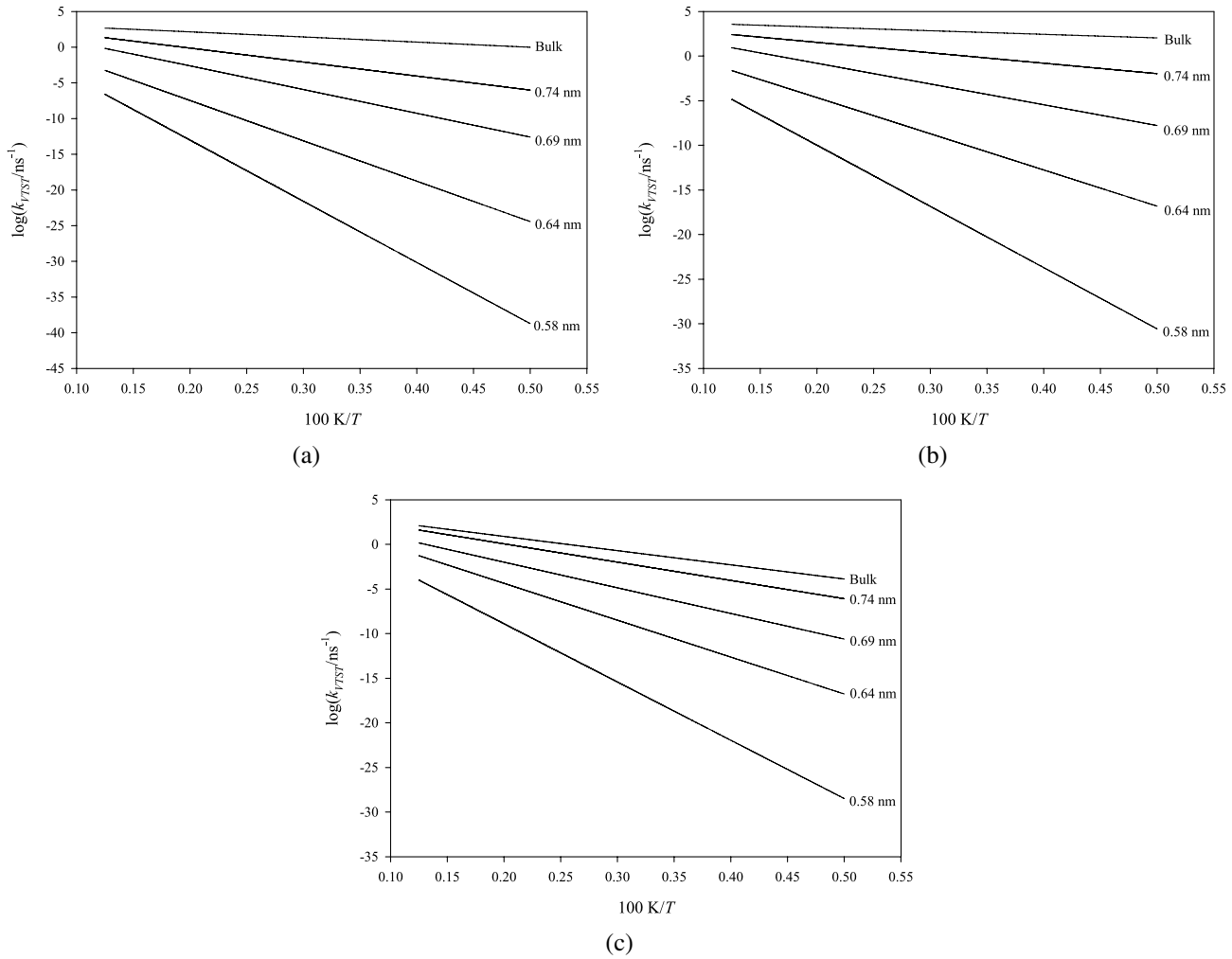

Fig. 2 Effect of confinement on the isomerization rates of n-butane (**a**), 1-butene (**b**), and 1,3-butadiene (**c**) as obtained from VTST calculations. The lines labeled "*Bulk*" corresponds to the isolated molecule (ideal gas). The *other lines* correspond to isolated molecules confined in carbon slit pores. The *labels next to the lines* indicate the corresponding pore widths

0.58 nm-wide pore. The variation is still over more than 20 orders of magnitude.

Finally, the results for 1,3-butadiene follow the same trends described above. Since this is the smallest molecule considered, the larger part of the variation in the rates happens at smaller pore widths than for n-butane and 1-butene, again reflecting that the important parameter is the molecular size compared to the characteristic size of the confining material. We still see, however, extreme variations of the rate with pore width, with the characteristic time for the *s-trans* → *gauche/s-trans* → *s-cis* transition at 300 K varying from 17 ns in the bulk to over 12 years in the smallest pore, a change of 16 orders of magnitude.

In our previous study of the asymmetric isomerization of n-butane using TST (Santiso et al. 2007a), we offered a simple explanation for this extreme variation of the rates with pore width, which we briefly reproduce here. The energy E_{ov} due to the overlap of the electron clouds of the confined molecule and the pore walls can, as a first approximation, be assumed to depend exponentially on the pore size r in the molecular sieving (small r) limit (Santiso et al. 2007a; Buckingham 1938):

$$E_{ov} \approx P \exp(-r/\rho) \tag{1}$$

In (1), the parameter P is a measure of the strength of the overlap interaction, and ρ is a measure of the length scale at which this interaction is relevant, which is directly related to the molecular size. In all the reactions considered the starting conformation is planar, whereas the transition state is non-planar, and thus the strongest overlap interaction should be the one with the transition state. If we neglect the overlap energy of the reactant compared to the one of the transition state, we obtain for the activation barriers:

$$\Delta E^{\ddagger} \approx \Delta E^{\ddagger}_{\infty} + P \exp(-r/\rho) \tag{2}$$

In (2), $\Delta E^{\ddagger}$ is the activation barrier within the pore, $\Delta E^{\ddagger}_{\infty}$ is the corresponding value in the bulk, and the parameters P and ρ are those for the transition state species. We can now invoke TST or assume an Arrhenius behavior for the isomerization kinetics—in either case the rate constant would be predicted to depend exponentially on the activation barrier, and therefore:

$$\begin{aligned} k &= A \exp\left[-\frac{\Delta E^{\ddagger}_{\infty} + P \exp(-r/\rho)}{k_B T}\right] \\ &= A' \exp[-P' \exp(-r/\rho)] \end{aligned} \tag{3}$$

The parameter A in (3) is a frequency factor, and we have defined the new temperature-dependent parameters $A' \equiv A \exp(-\Delta E^{\ddagger}_{\infty}/k_B T)$ and $P' \equiv P/k_B T$. This simple theory predicts that, when the overlap interaction is the most important contribution, the transition rate changes as the exponential of the exponential (i.e. the double exponential) of the pore size, which explains the extreme variations shown in Fig. 2.

We can eliminate the parameter A' by taking the bulk system as a reference, and rewrite (3) as:

$$\frac{k_{\infty}}{k} = \exp[P' \exp(-r/\rho)] \Rightarrow \ln\left(\ln \frac{k_{\infty}}{k}\right) = \ln P' - \frac{r}{\rho} \tag{4}$$

This predicts that a plot of $\ln[\ln(k_{\infty}/k)]$ vs. pore size should be approximately linear. In Fig. 3 we present such plots for the three isomerization reactions at 300 K using the data from Fig. 2. In all three cases the plot shows an approximately linear behavior, although the agreement is slightly better for n-butane and 1-butene ($R^2 = 0.99$) than it is for 1,3-butadiene ($R^2 = 0.97$). In the latter case, the larger deviation from the linear behavior comes from the point at the largest pore size (0.74 nm), where it is likely that the steric hindrance from the pore walls is not the only important contribution. Nevertheless, considering the simplicity of the theory behind (4), the agreement seen in Fig. 3 is remarkably good. We expect that such a dependence of kinetics on pore size will be found for any system where the overlap interaction dominates over other factors, and for which the Arrhenius equation is an adequate representation of the variation of the rate with the activation barrier. This includes most systems in which the characteristic dimensions of the confining material are comparable to the molecular size.

4 Concluding remarks

The results presented in this work show that the isomerization dynamics of n-butane, 1-butene and 1,3-butadiene are dramatically affected by confinement in the molecular sieving limit, i.e. when the pore size of the confining material becomes comparable to the molecular size. In spite of the differences in the bonding structure of the three molecules considered, they all show the same behavior within the smallest pores—their torsional potentials shift to an *anti-syn* (or *cis-trans*) form, and the isomerization rates vary by many orders of magnitude in a very narrow range of pore sizes. Our results are consistent with a double exponential dependence of the reaction rate with pore width, independently of the details of the confined molecule. We expect this type of behavior to be seen in most systems where the overlap interaction with the pore walls is the dominant interaction, i.e. for sufficiently small pore sizes. If this is indeed the case, this shape-catalytic effect could be used to design much improved catalytic supports using flexible materials such as graphitic carbon.

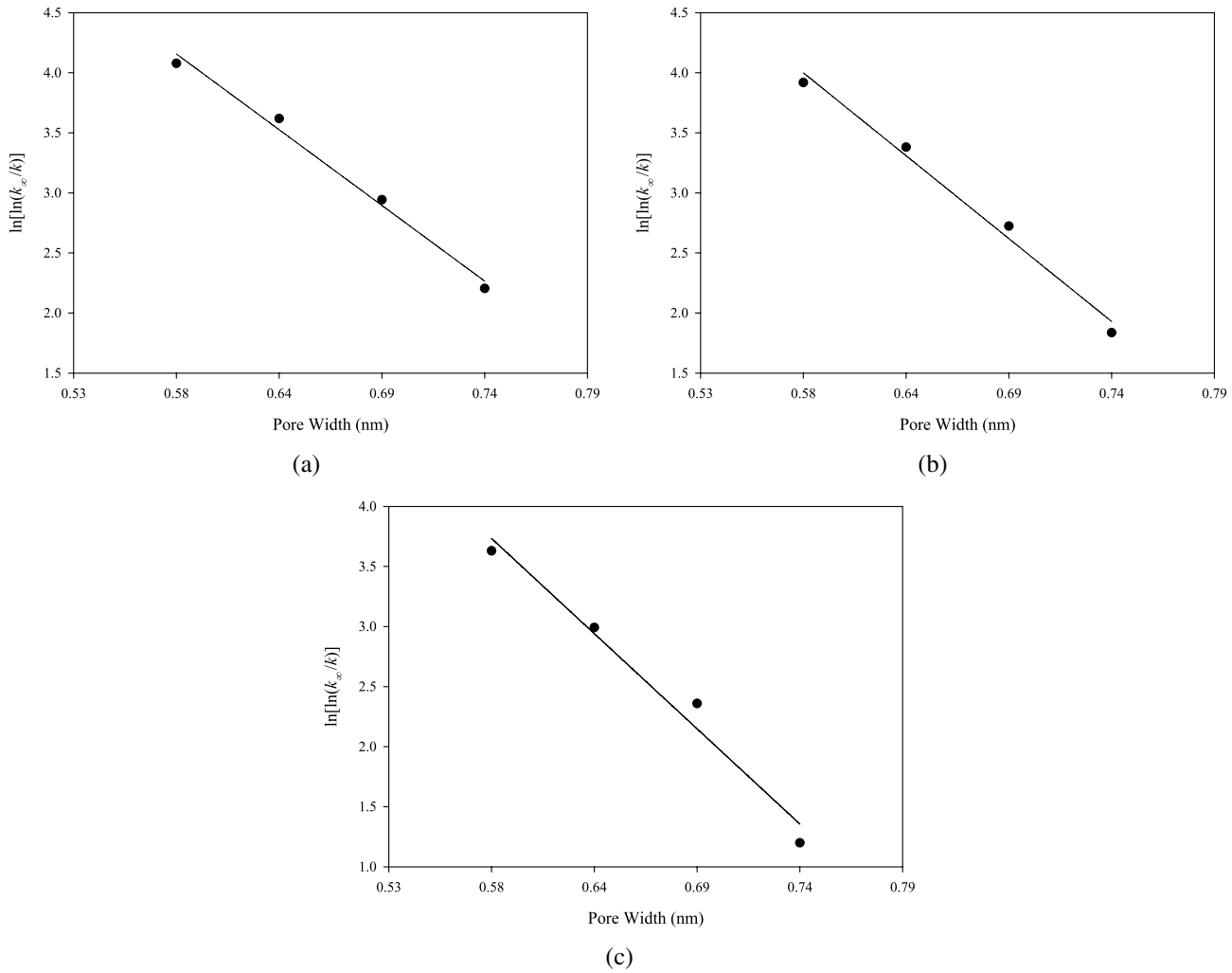

Fig. 3 The double exponential effect: plots of $\ln[\ln(k_\infty/k)]$ vs. pore width at 300 K for n-butane (**a**), 1-butene (**b**), and 1,3-butadiene (**c**) using the data from Fig. 2. The *black circles* correspond to our calculation results, and the *lines* are linear fits to the data. See discussion in the text

Acknowledgements We would like to acknowledge Aaron M. George, Sujata Paul and Liping Huang for helpful discussions. This work has been supported in part by: ACS-PRF; NSF (DMF-0304299 and CTS-0626031); BES, U.S. DOE at ORNL (DE-FG02-98ER14847 and DE-AC05-00OR22725 with UT-Battelle, LLC). Calculations have been carried out at CCS-ORNL, NCSU-HPC and San Diego and Pittsburgh Supercomputing Centers (NSF/NRAC NPA205). The molecular graphics in this work were created using Visual Molecular Dynamics (VMD) (Humprey et al. 1996).

References

Bandosz, T.J., Biggs, M.J., Gubbins, K.E., Hattori, Y., Iiyama, T., Kaneko, K., Pikunic, J., Thomson, K.T.: Molecular models of porous carbons. Chem. Phys. Carbon **28**, 41–228 (2003)

Bandow, S., Kokai, F., Takahashi, K., Yudasaka, M., Qin, L.C., Ijima, S.: Interlayer spacing anomaly of single-wall carbon nanohorn aggregate. Chem. Phys. Lett. **321**, 514–519 (2000)

Banerjee, A., Adams, N., Simons, J.: Search for stationary-points on surfaces. J. Phys. Chem. **89**, 52–57 (1985)

Becke, A.D.: Density-functional exchange-energy approximation with correct asymptotic-behavior. Phys. Rev. A **38**, 3098–3100 (1988)

Berber, S., Kwon, Y.K., Tomanek, D.: Electronic and structural properties of carbon nanohorns. Phys. Rev. B **62**, R2291–R2294 (2000)

Billeter, S.R., Curioni, A., Andreoni, W.: Efficient linear scaling geometry optimization and transition-state search for direct wavefunction optimization schemes in density functional theory using a plane-wave basis. Comp. Mater. Sci. **27**, 437–445 (2003)

Brown, D., Clarke, J.H.R.: Kinetics of isomerization in n-butane. J. Chem. Phys. **92**, 3062–3072 (1990a)

Brown, D., Clarke, J.H.R.: Rate constants from molecular dynamics. J. Chem. Phys. **93**, 4117–4122 (1990b)

Buckingham, R.A.: The classical equation of state of gaseous helium, neon and argon. Proc. Roy. Soc. London **167**, A264–A283 (1938)

Byl, O., Kondratyuk, P., Yates, J.T.: Adsorption and dimerization of NO inside single-walled carbon nanotubes—an infrared spectroscopy study. J. Phys. Chem. B **107**, 4277–4279 (2003)

El-Barbary, A.A.: First principles characterisation of defects in irradiated graphitic materials, Ph.D. Thesis, University of Sussex (2005)

Dresselhaus, M.S., Dresselhaus, G., Eklund, P.C.: Science of Fullerenes and Carbon Nanotubes. Academic Press, San Diego (1995)

González, J., Giménez, X., Bofill, J.M.: Generalized reaction-path Hamiltonian dynamics. Theor. Chem. Acc. **112**, 75–83 (2004)

Gray, C.G., Gubbins, K.E.: Fundamentals. Molecular Theory of Fluids, vol. 1. Clarendon, Oxford (1984)

Frenkel, D., Smit, B.: Understanding Molecular Simulation: From Algorithms to Applications, 2nd edn. Academic Press, San Diego (2002)

Halls, M.D., Schlegel, H.B.: Chemistry inside carbon nanotubes: the Menshutkin S_N2 reaction. J. Phys. Chem. B **106**, 1921–1925 (2002)

Hashimoto, A., Suenaga, K., Gloter, A., Urita, K., Iijima, S.: Direct evidence for atomic defects in graphene layers. Nature **430**, 870–873 (2004)

Humprey, W., Dalke, A., Schulten, K.: VMD: visual molecular dynamics. J. Mol. Graph. **14**, 33–38 (1996)

Imai, J., Souma, M., Ozeki, S., Suzuki, T., Kaneko, K.: Reaction of dimerized NO_x ($x = 1$ or 2) with SO_2 in a restricted slit-shaped micropore space. J. Phys. Chem. **95**, 9955–9960 (1991)

Kaneko, K., Fukuzaki, N., Kakei, K., Suzuki, T., Ozeki, S.: Enhancement of NO dimerization by micropore fields of activated carbon-fibers. Langmuir **5**, 960–965 (1989)

Kostov, M.K., Santiso, E.E., George, A.M., Gubbins, K.E., Buongiorno Nardelli, M.: Dissociation of water on defective carbon substrates. Phys. Rev. Lett. **95**, Art. No. 136105 (2005)

Lee, C., Yang, W., Parr, R.G.: Development of the Colle-Salvetti correlation-energy formula into a functional of the electron-density. Phys. Rev. B **37**, 785–789 (1988)

Lisal, M., Brennan, J.K., Smith, W.R.: Chemical reaction equilibrium in nanoporous materials: NO dimerization reaction in carbon slit nanopores, J. Chem. Phys. **124**, Art. No. 064712 (2006)

Page, M., McIver, J.W., Jr.: On evaluating the reaction path Hamiltonian. J. Chem. Phys. **88**, 922 (1988)

Parr, R.G., Yang, W.: Density-Functional Theory of Atoms and Molecules. Oxford University Press, Oxford (1989)

Reed, T.M., Gubbins, K.E.: Applied Statistical Mechanics. McGraw-Hill, New York (1973)

Santiso, E.E., Gubbins, K.E.: Multi-scale molecular modeling of chemical reactivity. Mol. Simul. **30**, 699–748 (2004)

Santiso, E.E., George, A.M., Turner, C.H., Kostov, M.K., Gubbins, K.E., Buongiorno Nardelli, M., Sliwinska-Bartkowiak, M.: Adsorption and catalysis: the effect of confinement on chemical reactions. Appl. Surf. Sci. **252**, 766–777 (2005a)

Santiso, E.E., George, A.M., Sliwinska-Bartkowiak, M., Buongiorno Nardelli, M., Gubbins, K.E.: Effect of confinement on chemical reactions. Adsorption **11**, 349–354 (2005b)

Santiso, E.E., George, A.M., Gubbins, K.E., Buongiorno Nardelli, M.: Effect of confinement by porous carbons on the unimolecular decomposition of formaldehyde. J. Chem. Phys. **125**, Art. No. 084711 (2006)

Santiso, E.E., Buongiorno Nardelli, M., Gubbins, K.E.: A remarkable shape-catalytic effect of confinement on the rotational isomerization rate of small hydrocarbons. J. Chem. Phys. (2007a, in press)

Santiso, E.E., Kostov, M.K., George, A.M., Buongiorno Nardelli, M., Gubbins, K.E.: Confinement effects on chemical reactions—toward an integrated rational catalyst design. Appl. Surf. Sci. **253**, 5570–5579 (2007b)

Simons, J.: An Introduction to Theoretical Chemistry. Cambridge University Press, Cambridge (2003)

Travis, K.P., Searles, D.J.: Effect of solvation and confinement on the *trans-gauche* isomerization reaction in n-butane. J. Chem. Phys. **125**, Art. No. 164501 (2006)

Turner, C.H., Gubbins, K.E.: Effects of supercritical clustering and selective confinement on reaction equilibrium: a molecular simulation study of the esterification reaction. J. Chem. Phys. **119**, 6057–6067 (2003)

Turner, C.H., Pikunic, J., Gubbins, K.E.: Influence of chemical and physical surface heterogeneity on chemical reaction equilibria in carbon micropores. Mol. Phys. **99**, 1991–2001 (2001a)

Turner, C.H., Johnson, J.K., Gubbins, K.E.: Effect of confinement on chemical reaction equilibria: the reactions $2NO \leftrightarrow (NO)_2$ and $N_2 + 3H_2 \leftrightarrow 2NH_3$ in carbon micropores. J. Chem. Phys. **114**, 1851–1859 (2001b)

Turner, C.H., Brennan, J.K., Johnson, J.K., Gubbins, K.E.: Effect of confinement by porous materials on chemical reaction kinetics. J. Chem. Phys. **116**, 2138–2148 (2002)

Vanderbilt, D.: Soft self-consistent pseudopotentials in a generalized eigenvalue formalism. Phys. Rev. B **41**, 7892–7898 (1990)